Journal of Pharmaceutical Analysis 11 (2021) 764–775

Contents lists available at ScienceDirect

Journal of Pharmaceutical Analysis

journal homepage: www.elsevier.com/locate/jpa

Original article

Impaired tricarboxylic acid cycle flux and mitochondrial aerobic respiration during isoproterenol induced myocardial ischemia is rescued by bilobalide

Zhe Wang [1], Fan Zhang [1], Wei Liu [1], Ning Sheng, Hua Sun**, Jinlan Zhang*

State Key Laboratory of Bioactive Substance and Function of Natural Medicines, Institute of Materia Medica, Chinese Academy of Medical Sciences & Peking Union Medical College, Beijing, 100050, China

ARTICLE INFO

Article history:
Received 10 March 2020
Received in revised form
12 August 2020
Accepted 13 August 2020
Available online 26 August 2020

Keywords:
Bilobalide
Isoproterenol-induced myocardial ischemia
Tricarboxylic acid cycle
Stable isotopic tracing metabolic flux analysis
Seahorse test

ABSTRACT

There is an urgent need to elucidate the pathogenesis of myocardial ischemia (MI) and potential drug treatments. Here, the anti-MI mechanism and material basis of *Ginkgo biloba* L. extract (GBE) were studied from the perspective of energy metabolism flux regulation. Metabolic flux analysis (MFA) was performed to investigate energy metabolism flux disorder and the regulatory nodes of GBE components in isoproterenol (ISO)-induced ischemia-like cardiomyocytes. It showed that [U−^{13}C] glucose derived m+2 isotopologues from the upstream tricarboxylic acid (TCA) cycle metabolites were markedly accumulated in ISO-injured cardiomyocytes, but the opposite was seen for the downstream metabolites, while their total cellular concentrations were increased. This indicates a blockage of carbon flow from glycolysis and enhanced anaplerosis from other carbon sources. A Seahorse test was used to screen for GBE components with regulatory effects on mitochondrial aerobic respiratory dysfunction. It showed that bilobalide protected against impaired mitochondrial aerobic respiration. MFA also showed that bilobalide significantly modulated the TCA cycle flux, reduced abnormal metabolite accumulation, and balanced the demand of different carbon sources. Western blotting and PCR analysis showed that bilobalide decreased the enhanced expression of key metabolic enzymes in injured cells. Bilobalide's efficacy was verified by in vivo experiments in rats. This is the first report to show that bilobalide, the active ingredient of GBE, protects against MI by rescuing impaired TCA cycle flux. This provides a new mechanism and potential drug treatment for MI. It also shows the potential of MFA/Seahorse combination as a powerful strategy for pharmacological research on herbal medicine.

1. Introduction

Myocardial ischemia (MI) is a major threat to human health worldwide and there is an urgent need to study its pathogenesis and treatment [1]. MI is a metabolic disorder characterized by enhanced glycolysis, inhibition of glucose aerobic oxidation, and reduced ATP production [2–4]. Therefore, myocardial energy metabolism is an important target for the prevention and treatment of MI. At present, the main effects of drugs targeting myocardial energy metabolism are in inhibiting the intake and oxidation of free fatty acids and increasing the utilization of glucose [5,6]. In addition, the tricarboxylic acid (TCA) cycle is the hub of carbohydrate, lipid and amino acid metabolism and provides most of the energy for biological activities. The fluency of the TCA cycle is very important, because the steady state concentrations of its intermediates are typically low in relation to the fluxes through it [7]. It has been reported that after ischemia, the TCA cycle flux in cardiomyocytes changes; succinate and fumarate accumulate, and the reductive carboxylation of glutamine is enhanced [8]. However, measurement of the TCA cycle flux is technically challenging, and therapeutic drugs for altering metabolic flux have not been found.

Ginkgo biloba L. extract (GBE) has been widely used in the prevention and treatment of ischemic heart disease (IHD) for decades [9]. However, its metabolic regulatory mechanism in MI is still unclear. Isoproterenol (ISO)-induced MI is an important MI model for pathological and pharmacological research. ISO is a β-receptor

Peer review under responsibility of Xi'an Jiaotong University.
* Corresponding author.
** Corresponding author.
E-mail addresses: sunhua@imm.ac.cn (H. Sun), zhjl@imm.ac.cn (J. Zhang).
[1] These authors contributed equally to this work.

https://doi.org/10.1016/j.jpha.2020.08.008

agonist that can induce a state similar to hypoxic-ischemic injury in cardiomyocytes [10]. Therefore, we developed a metabolomics study of GBE protection against ISO-induced MI in rats [11]. In that previous study, we demonstrated that GBE significantly improves myocardial lipid, amino acid, and energy metabolism disorders caused by ischemia. GBE's regulation of energy metabolism attracted our attention because energy metabolism is very important for the heart, which needs sufficient energy to support its continuous activity. It was observed that GBE significantly reduces the accumulation of citrate in the myocardium due to TCA cycle dysfunction. Additionally, four amino acids significantly increase after MI and are metabolized as intermediates to enter and maintain the TCA cycle. GBE significantly downregulates the levels of these amino acids. This study showed that GBE enhances the metabolic fluency of TCA cycle intermediates and reduces their accumulation, and these interesting findings cannot be explained by the currently reported mechanisms. This suggests that GBE is a potential source of a therapeutic drug to effect metabolic flux. Furthermore, we identified nine prototypes and six metabolites of GBE in the rat heart. In this paper, we explore the material basis of GBE and how it protects against MI.

Many metabolites participate in multiple pathways, and although they may exhibit significant changes in a certain pathway, their overall measured concentrations may not change [12]. Stable isotopic tracing metabolic flux analysis (MFA) introduces tracers (containing ^{13}C, ^{15}N, or ^{2}H) into the biological system, which results in changes in the isotope distribution patterns of downstream metabolites. By liquid chromatography-mass spectrometry (LC-MS) analysis, the isotope incorporation ratio and content of these metabolites over time can be detected to identify metabolic switching and changes in the sources, rates, and directions of metabolites, providing a more in-depth and accurate portrayal of the metabolic process [13]. In addition, the Seahorse test as a real-time monitoring technique can characterize the energy metabolism phenotypes of living cells under pathological and normal states and verify metabolic sites and pathways [14]. Some valuable research [15–17] has been carried out on MFA assisted by the Seahorse test that focuses on the dynamic changes in cellular energy metabolism, especially in studies assessing the mechanism of medicines. For example, with these two techniques, a clinical-grade potential drug, IACS-010759, was discovered. It robustly inhibits proliferation and induces apoptosis in brain cancer and acute myeloid leukaemia, owing to a combination of energy depletion and reduced aspartate production that leads to impaired nucleotide biosynthesis [16]. Therefore, the MFA/Seahorse test combination provides a new strategy to expand our metabolomics research.

The search for drugs that affect myocardial energy metabolism for MI therapy is very popular right now. However, because measuring metabolic flux is technically challenging, this kind of drug is hard to find. In our previous study, we found that GBE enhances the metabolic fluency of the TCA cycle, suggesting that GBE has the potential as a source of therapeutic drugs to alter metabolic flux through a new strategy composed of the MFA technique and Seahorse test. In the present study, as shown in Fig. 1, the Seahorse test was used to screen GBE monomers with regulatory effects on the mitochondrial aerobic respiratory dysfunction of ISO-injured H9c2 cells. The stable isotope MFA technique was used to study metabolic energy flux disorder in injured cardiomyocytes and the exact regulatory nodes of the active monomer, along with the corresponding metabolic enzymes. The expression of these key enzymes was analyzed by an RT2 profiler PCR assay and Western blotting. Finally, in vivo experiments in rats were used for further verification. Through the above workflow, we found a blockage of carbon flow from glycolysis to the TCA cycle and enhanced anaplerosis from other carbon sources in ISO-injured cells. For the first time, bilobalide was identified as having a good effect on modulating mitochondrial aerobic respiration and TCA cycle flux. Bilobalide caused decreases in the expression of key enzymes in energy metabolism in injured cells. As the active compound of GBE, bilobalide not only provides further proof of the pathological metabolic mechanism of MI but also serves as an inspiration for new drug discovery. This work with bilobalide also shows the potential of the Seahorse test combined with the MFA technique as a powerful strategy for research on herbal medicine mechanisms.

2. Experimental

2.1. Reagents and chemicals

Bilobalide, ginkgolide A, ginkgolide B, ginkgolide C, quercetin, isorhamnetin, kaempferol, apigenin, and rutin (purity > 98.0%, Baoji Herbest Bio-Tech Co., Ltd., Baoji, China); diltiazem (Tianjin, Tanabe Seiyaku, Co., Ltd., Tianjin, China); all metabolite standards (Sigma-Aldrich, St. Louis, MO, USA; J&K Scientific, Beijing, China); isotope labelled internal standards and [U–^{13}C] glucose tracers (Cambridge Isotope, Woburn, MA, USA); methanol (Fisher

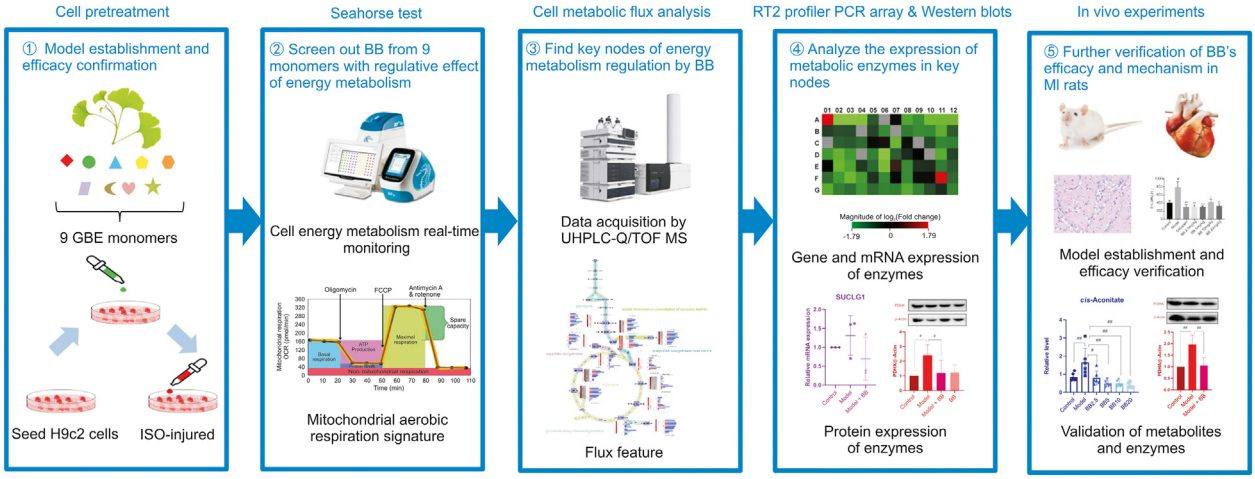

Fig. 1. The workflow of this study. GBE: *Ginkgo biloba* L. extract; ISO: isoproterenol; BB: bilobalide; MI: myocardial ischemia.

Scientific, Fair Lawn, NJ, USA); ISO, formic acid, and *N*,*N*-dimethyloctylamine (Sigma-Aldrich, St. Louis, MO, USA); Ultra-pure water (Milli-Q purification system, Millipore, Bedford, MA, USA); Dulbecco's modified Eagle's medium (DMEM) and fetal bovine serum (FBS) (National Infrastructure of Cell Line Resource, Beijing, China); penicillin/streptomycin mixture (100 U/mL: 100 μg/mL, Beijing Solarbio Science & Technology Co., Ltd., Beijing, China); L-glutamine (Life Technologies, Carlsbad, CA, USA); bicinchoninic acid (BCA) Protein Assay Kit and super electrochemiluminescence detection reagent (Applygen Technologies Inc., Beijing, China); creatine kinase (CK)-MB standard kit (BioSino Biotechnology Co., Ltd., Beijing, China); anti-IDH2 (Abcam, Cambridge, UK, Cat# ab131263, RRID: AB_11156098); anti-β-tubulin (Zsjqbio, Beijing, China, Cat# TA-10); anti-ACTB (Cat# AC026, RRID: AB_2768234), horseradish peroxidase (HRP) Goat Anti-Rabbit IgG (Cat# AS014, RRID: AB_2769854), HRP Goat Anti-Mouse IgG (Cat# AS003, RRID: AB_2769851), anti-CS (Cat# A5713, RRID: AB_2766471), anti-PDHX (Cat# A6426, RRID: AB_2767028), anti-PDHA (Cat# A17432, RRID: AB_2770834), anti-SDHB (Cat# A10821, RRID: AB_2758247), and anti-SUCLG1 (Cat# A15345, RRID: AB_2762247) from ABclonal Technology Co., Ltd. (Wuhan, China); XFe24 Cell Mito Stress Test Kit, Seahorse XFe24 Calibrant, and Seahorse XFe24 medium (Agilent Seahorse, Billerica, MA, USA); and RNeasy® Mini Kit, RT2 Profiler PCR Array, RT2 First Strand Kit, and RT2 SYBR Green qPCR Mastermix (QIAGEN, Hilden, Germany).

2.2. Cell lines and culture

H9c2 cells (BCRC, Cat# 60096, RRID: CVCL_0286) were maintained at 37 °C with 5% CO_2 in DMEM, supplemented with 10% FBS, 1% penicillin/streptomycin, and 4 mmol/L L-glutamine. The cells were seeded in 96-well plates, treated with ISO and/or GBE monomers for 24 h, and tested for cell viability with a Cell Counting Kit-8 (CCK-8).

2.3. Seahorse respirometry test

Cellular oxygen consumption rate (OCR) was measured using an XFe24 Extracellular Flux Analyser (Agilent Seahorse, Billerica, MA, USA) and the Mito Stress Test Kit, according to the manufacturer's protocol. H9c2 cells (2×10^5) were plated in 100 μL of their standard growing media and cultured overnight. On the day of measurement, cells were washed with XFe24 media and incubated in a CO_2-free incubator at 37 °C for 2 h to establish equilibration prior to loading. OCR measurements were obtained before and after addition of glucose (10 mmol/L), oligomycin (1 μmol/L), FCCP (4 μmol/L), and rotenone/antimycin A (0.5 μmol/L). These measurements were used to calculate basal respiration, ATP production, and maximal respiration.

2.4. Cell treatment for metabolic flux analysis

H9c2 cells were seeded in growth media at 5×10^5 cells per dish and divided into five groups: ^{12}C control group, ^{13}C control group, MI model group, bilobalide control group, and bilobalide + MI model group. After 24 h of cell culture, the medium in each dish except for the ^{12}C control group were exchanged with an isotope tracing medium consisting of glucose-free DMEM supplemented with 25 mmol/L [U−^{13}C] glucose. Bilobalide (10 μmol/L) was added in the culture medium of the bilobalide group and bilobalide + MI model group with DMSO as the vehicle. After another 24 h of cell culture, 600 μmol/L ISO was added to the MI model group and bilobalide + MI model group with DMSO as the vehicle. After 6 h of cell culture, cells were harvested for MFA. Cells in the ^{12}C control group were incubated with media supplemented with 25 mmol/L unlabelled glucose and harvested at the same time. This experiment was repeated independently three times.

2.5. UHPLC-HRMS isotope tracing metabolic flux analysis

The culture medium was gently aspirated and cells were collected in a glass centrifuge tube. After adding 20 μL of d8-phenylalanine internal standard solution and 1 mL of cooled methanol:water (80:20, *V/V*) solution, the cells were extracted by ultrasound and vortex for 1 min. The centrifuge tubes were incubated at −80 °C for 2 h to aid protein precipitation, exposed to ultrasound, and vortexed again for 1 min. After centrifugation at 12,470 *g* for 5 min at 4 °C, the supernatant was transferred to another glass centrifuge tube and dried under a gentle nitrogen stream and then kept at −80 °C. Dried extracts were re-suspended in 120 μL of water and incubated on ice for 20 min, and vortexed every 5 min. After centrifugation at 12,470 *g* for 5 min at 4 °C, a 100 μL of supernatant was transferred to an auto-sampler vial, and 10 μL was removed from each sample to prepare a pooled quality control sample that was injected six times at the start of the analytical run and then quality control regularly throughout the batch.

LC separation was performed using an Agilent 1290 UPLC system (Agilent, Santa Clara, CA, USA) and CORTECS C_{18} column (2.1 mm × 150 mm, 2.7 μm; Waters, Milford, MA, USA). Mobile phase A was water:methanol (90:10, *V/V*) with 5 mmol/L *N*,*N*-dimethyloctylamine and 0.04% formic acid. Mobile phase B was water:-methanol (10:90, *V/V*) with 5 mmol/L *N*,*N*-dimethyloctylamine and 0.04% formic acid. The injection volume was 15 μL and the LC gradient condition was 0–4 min, 0%–20% B; 4–8 min, 20%–100% B; 8–10 min, 100% B with 5 min of re-equilibration time, flow rate was 0.4 mL/min on 0–8 min and 0.6 mL/min on 8.1–10 min. The column temperature was 30 °C. MS detection was performed using an Agilent 6550 Q-TOF mass spectrometer (Agilent, Santa Clara, CA, USA) with Dual Jet Stream ESI source operating in negative ionization mode. MS parameters were dry gas temperature, 200 °C; dry gas flow, 14 L/min; nebulizer pressure, 35 psi; sheath gas temperature, 350 °C; sheath gas flow, 11 L/min; capillary voltage, −3.5 kV; nozzle voltage, −600 V; VCap, 3500 V; fragmentor, 380 V; and octopole radiofrequency, 750 V. Active reference mass correction was through a second nebulizer using masses with *m*/*z* 112.985587 and 1033.988109. Data were acquired from *m*/*z* 50–1200 with an acquisition rate of 1.5 spectra/s at a high-resolution mode of 2 GHz Ext Dyn Range. The metabolite database of the TCA cycle, glycolysis, and pentose phosphate pathway was established using MassHunter Pathways to PCDL and PCDL Manager software. Data analysis and isotopic natural abundance correction were performed within MassHunter VistaFlux and MassHunter Quant software.

2.6. RT2 profiler PCR array gene expression analysis

Total RNA was extracted from H9c2 cells treated with ISO and bilobalide using TRIzol (Invitrogen, Waltham, MA, USA) according to the manufacturer's specifications. The yield of RNA was determined using a NanoDrop 2000 spectrophotometer (Thermo Scientific, Waltham, MA, USA), and the integrity was evaluated using agarose gel electrophoresis with ethidium bromide staining. Then, quantification was performed with a two-step reaction process and reactions were performed in GeneAmp® PCR System 9700 (Applied Biosystems, Waltham, MA, USA). The expression levels of mRNAs were normalized to β-actin and were calculated using the $2^{-\Delta\Delta Ct}$ method.

2.7. Western blots

Cells were washed with ice-cold PBS and mixed with a moderate radio immune precipitation assay (RIPA) buffer to obtain lysates. Total protein in the supernatant was measured by using a BCA Protein Assay Kit. Lysates taken from each sample were separated by 12% SDS-PAGE, transferred to polyvinylidene difluoride membranes, blocked with 5% non-fat milk for 2 h at room temperature, and placed overnight at 4 °C with specific antibodies: PDHX, PDHA, CS, SUCLG1, SDHB, IDH2, and β-actin. After washing with 0.2% Tween-20 in Tris-buffered saline, the membranes were incubated with a HRP-conjugated secondary antibody at room temperature for 2 h. The reactive bands were visualized using ImageQuant LAS 4000 (GE Healthcare Bio-Sciences, AB, Uppsala, Sweden). The optical density of signals on membranes was quantified using Gel-Pro Software. β-actin expression levels were measured in parallel to serve as controls.

2.8. Animal experiments

Thirty-five male SD rats (200 ± 15 g) were purchased from Vital River Laboratories Co., Ltd. (Beijing, China). The animals were housed under pathogen-free conditions of temperature (25 ± 2 °C), humidity (50% ± 5%) and light (12 h light/12 h dark cycle) with free access to food and water. The rats were given a week to acclimate before the experiments. All animal studies complied with guidelines and ethics of Chinese Academy of Medical Sciences and Peking Union Medical College, China.

Rats were divided randomly into seven groups of five rats, which were control rats (group A), MI model rats (group B), MI model rats pre-treated with diltiazem (50 mg/kg, i.p., equivalent to the clinical dose used in humans, group C), and MI model rats pre-treated with bilobalide (2.5, 5, 10, and 20 mg/kg, i.p., groups D to G). Pre-treated rats were administered drug for 7 consecutive days. On the 6th and 7th days, rats in groups B to G received two injections of ISO (40 mg/kg, s.c.) to establish the MI model, and group A received saline for control. The rats were sacrificed on the 8th day after euthanasia (10% chloral hydrate, 0.33 mL/100 g, i.p.), and blood samples were collected through the abdominal aorta using heparin as an anticoagulant. Plasma was obtained by centrifugation (664 *g*, 15 min) and kept at −80 °C.

Hearts were excised, washed with cold saline, and cut. A half of the heart was fixed in 10% buffered formalin for histopathological examination. The other half was kept at −80 °C for further evaluation. Part of the heart tissue samples were homogenized in saline at a 1:10 ratio of tissue to solution. Another part of the heart was mixed with a moderate RIPA buffer to obtain lysates, which were analyzed with Western blot and cell sample experiments. The level of CK-MB in plasma and the protein content of heart homogenates were determined using their standard kits respectively.

2.9. Targeted metabolomic profiling

Tissue homogenate (100 μL) was transferred into a 2 mL Eppendorf tube and added to 20 μL of d8-phenylalanine internal standard solution. After being vortexed for 10 s, 1 mL of acetonitrile was added to the tube, the sample was vortexed for 5 min, and centrifuged at 12,470 *g* for 10 min at 4 °C. The supernatant was transferred into a glass centrifuge tube and dried under a gentle nitrogen stream. The residue was re-dissolved in 100 μL of acetonitrile:methanol (75:25, *V/V*) solution for testing. A 5 μL aliquot was used for Agilent 6490 Triple Quadrupole LC-MS (Agilent, Santa Clara, CA, USA) testing to analyze metabolites in the TCA cycle and glycolysis. LC separation was performed using a Waters XBridge Amide column (2.1 mm × 50 mm, 1.7 μm; Waters, Milford, MA, USA). Mobile phase A was acetonitrile:water (50:50, *V/V*) with 15 mmol/L ammonium acetate and 0.2% ammonium hydroxide. Mobile phase B was acetonitrile:water (95:5, *V/V*) with 15 mmol/L ammonium acetate and 0.2% ammonium hydroxide. The gradient condition was 0–1 min, 95%–74% B; 1–4 min, 74%–53% B; and 4–8 min, 53% B with 4 min of re-equilibration time. The flow rate was 0.3 mL/min. The column temperature was 35 °C. MS detection was performed using an AJS electrospray ionization interface to the tandem MS. The operating parameters were dry gas temperature, 200 °C; dry gas flow rate, 14 L/min; nebulizer pressure, 20 psi; sheath gas temperature, 250 °C; sheath gas rate, 11 L/min; capillary voltage, −3.0 kV, and nozzle voltage, −1.5 kV. Multiple reaction monitoring was performed in negative ion mode using the precursor-to-product ion transitions, fragmentor voltage (380 V), and collision energies. Data analysis was performed within MassHunter Quant software.

2.10. Data and statistical analysis

The original data and images are shown in the Supplementary data. Quantitative data are presented as the mean ± SD and tested for normality with a Shapiro–Wilk test. Differences between two groups were analyzed by the Student's *t*-test for normal distribution data or Mann-Whitney test for non-normal distribution data. All statistical analyses were performed using GraphPad Prism software version 8.0.2 (GraphPad Software, Inc., San Diego, CA, USA, RRID: SCR_002798), and the level of significance was set at $P < 0.05$.

3. Results

3.1. Disturbed TCA cycle flux of ISO-induced ischemia-like cardiomyocytes

A UHPLC-HRMS method for isotope tracing metabolic flux analysis of energy metabolism was established, and the extracted ion chromatograms and mass spectra of metabolites detected in H9c2 cells cultured with [U−^{13}C] glucose are shown in Fig. S1. Cells reach both a metabolic and isotopic steady state as a precondition of stable isotope tracer MFA [15]. According to the cell growth rate, H9c2 cells reached the metabolic steady state at 24 h. Then, H9c2 cells were cultured with [U−^{13}C] glucose, and the time to reach an isotopic steady state was determined according to the change in the ^{13}C labelled ratio of metabolites over time. After 24 h of cell culture, the ^{13}C labelled ratio of metabolites in glycolysis and the TCA cycle pathway stabilized at approximately 15%–80%, which indicated that the isotopic steady state of the cells was reached and maintained at 24 h.

3.1.1. Glucose as a source of carbon in the TCA cycle was blocked in injured cardiomyocytes

As shown in Fig. 2A, [U−^{13}C] glucose was used as a tracer to study the energy metabolism of ISO-injured H9c2 cells. Metabolites in glycolysis derived from glucose were labelled as m+6 or m+3, whereas metabolites in the TCA cycle derived from glucose were labelled as m+2. As shown in Fig. 2B (Table S1), after culture with [U−^{13}C] glucose, model cells showed interesting changes compared with the changes in the control cells: ^{13}C labelled metabolites in the upstream TCA cycle were significantly increased, including m+2 isotopologues of citrate/isocitrate and *cis*-aconitate, whereas ^{13}C labelled metabolites in the downstream TCA cycle were significantly decreased, including m+2 isotopologues of α-ketoglutarate, succinate, fumarate, malate, and aspartate (representing oxaloacetate). This indicated that carbon source from glucose entering the TCA cycle was increased after ISO-induced injury, but blocked between isocitrate and α-ketoglutarate.

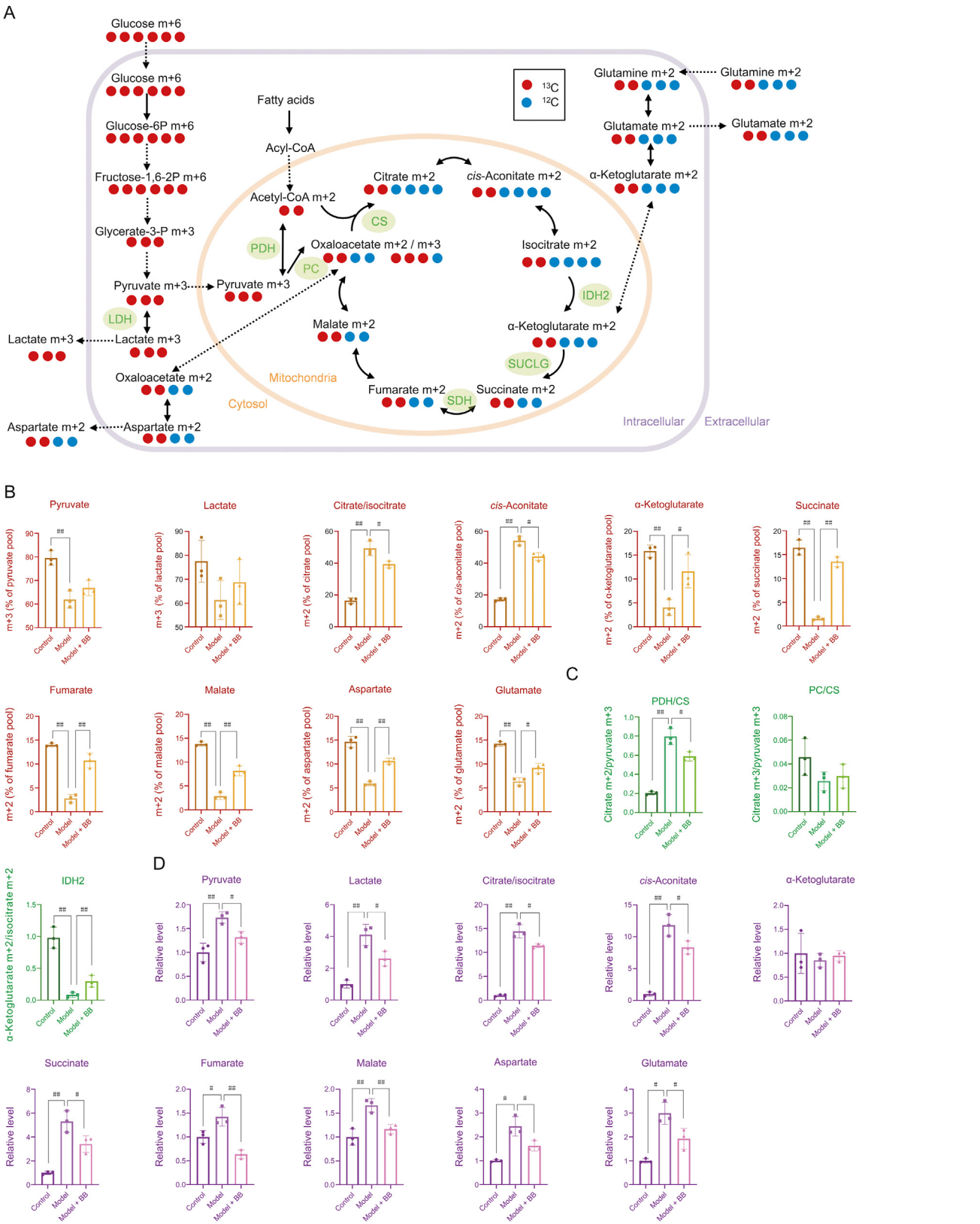

Fig. 2. (A) Schematic for the metabolism of [U−^{13}C] glucose. (B) ^{13}C labelling of each metabolite in energy metabolism (n=3. The original data are shown in Table S1). (C) PDH/CS, PC/CS and IDH2 activity calculated by ^{13}C labelling ratio of metabolites (n=3). (D) Total cellular concentration of each metabolite in energy metabolism (n=3. The original data are shown in Table S2). Error bars represent mean ± SD, $^{\#}P < 0.05$, $^{\#\#}P < 0.01$. PDH: pyruvate dehydrogenase; CS: citrate synthetase; PC: pyruvate carboxylase; IDH2: isocitrate dehydrogenase 2; BB: bilobalide.

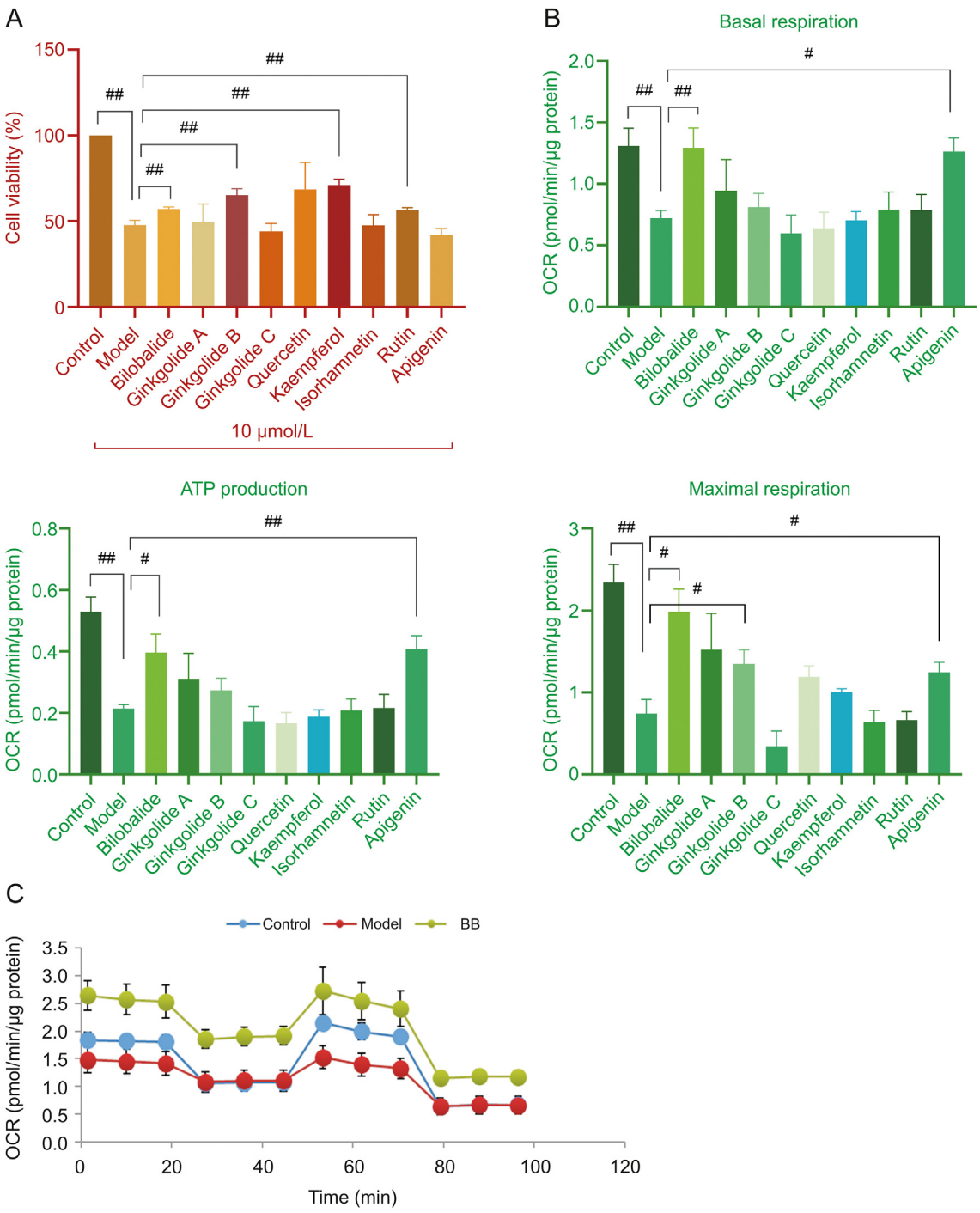

Fig. 3. (A) Effects of ISO and the main GBE monomers on H9c2 cell viability (n=3. The original data are shown in Table S3). (B) The basal respiration, ATP production, and maximal respiration of H9c2 cells treated with ISO and GBE monomers (n=6. The original data are shown in Tables S4–S6). (C) The mitochondrial respiration activity of H9c2 cells treated with ISO and bilobalide (n=6). Error bars represent mean ± SD, $^{\#}P < 0.05$, $^{\#\#}P < 0.01$. ISO: isoproterenol; OCR: oxygen consumption rate; BB: bilobalide.

Pyruvate from U–^{13}C glucose is also a carbon source for the TCA cycle via pyruvate dehydrogenase (PDH) and pyruvate carboxylase (PC). As shown in Fig. 2C, the citrate m+2/pyruvate m+3 ratio represents PDH and/or citrate synthetase (CS) activity, whereas the citrate m+3/pyruvate m+3 ratio represents PC activity [18]. As shown in Fig. 2C, the citrate m+2/pyruvate m+3 ratio was significantly increased after injury, which indicated an active PDH and/or CS activity. Additionally, PC activity was not significantly changed after injury, as shown by the lack of difference in the citrate m+3/pyruvate m+3 ratio. In the TCA cycle, isocitrate was converted to α-ketoglutarate by isocitrate dehydrogenase 2 (IDH2). The α-ketoglutarate m+2/isocitrate m+2 ratio, which represents IDH2 activity, was significantly decreased after injury, which indicated suppressed IDH2 activity. However, IDH2 is a rate-limiting enzyme in the TCA cycle. Possibly due to the significant increase of PDH and/or CS activity, the carbon sources entering the TCA cycle increased rapidly and significantly, and IDH2 could not catalyze the conversion of isocitrate into α-ketoglutarate in time, which resulted in the decreased α-ketoglutarate m+2/isocitrate m+2 ratio.

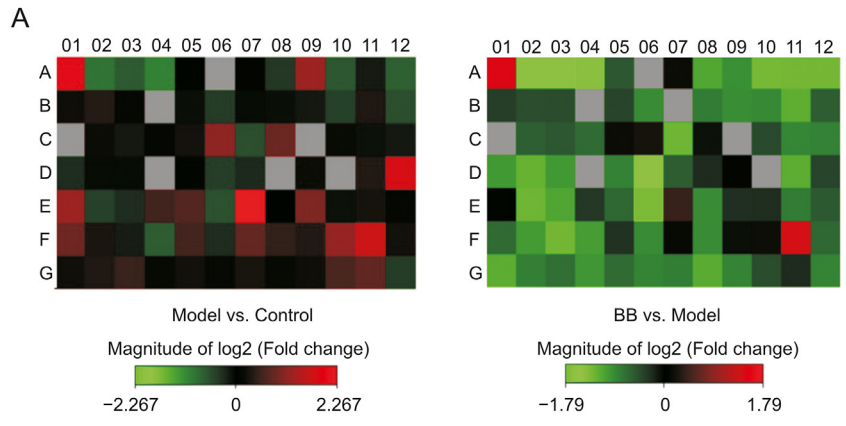

Layout	01	02	03	04	05	06	07	08	09	10	11	12
A	Acly	Aco1	Aco2	Agl	Aldoa	Aldob	Aldoc	Bpgm	Cs	Dlat	Dld	Dlst
B	Eno1	Eno2	Eno3	Fbp1	Fbp2	Fh	G6pc	G6pc3	G6pd	Galm	Gapdh	Gapdhs
C	Gck	Gpi	Gsk3a	Gsk3b	Gys1	Gys2	H6pd	Hk2	Hk3	Idh1	Idh2	Idh3a
D	Idh3b	Idh3g	Mdh1	Mdh1b	Mdh2	Ogdhl	Pc	Pck1	Pck2	Pdha2	Pdhb	Pdhx
E	Pdk1	Pdk2	Pdk3	Pdk4	Pdp2	Pdpr	Pfkl	Pgam2	Pgk1	Pgk2	Pgls	Pgm1
F	Pgm2	Pgm3	Phka1	Phkb	Phkg1	Phkg2	Pklr	Prps1	Prps1|1	Pygl	Pygm	Rbks
G	Rpia	Sdha	Sdhb	Sdhc	Sdhd	Sucla2	Suclg1	Suclg2	Taldo1	Tkt	Tpi1	Ugp2

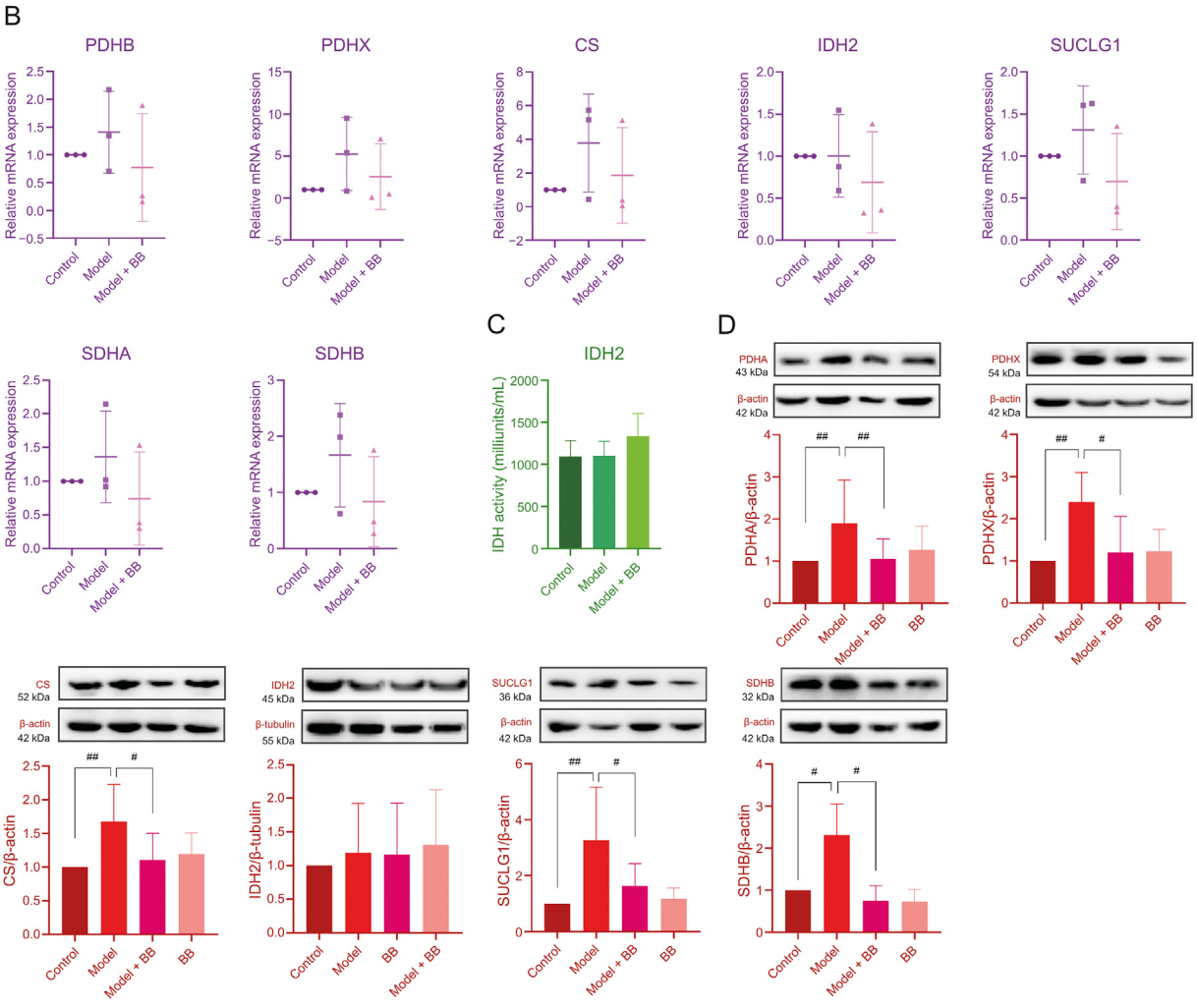

Fig. 4. (A) The gene expression levels of enzymes in energy metabolism. (B) The mRNA expression levels of some enzymes in energy metabolism (n=3. The original data are shown in Table S7). (C) The activity of IDH2 (n=3. The original data are shown in Table S8). (D) The protein expression levels of some enzymes involved in energy metabolism (n=3–15. The original data are shown in Figs. S2–S7). Error bars represent mean ± SD, $^{\#}P < 0.05$, $^{\#\#}P < 0.01$. PDHA, PDHB and PDHX are subunits of PDH. SUCLG1 is a subunit of SUCLG. SDHA and SDHB are subunits of SDH.

3.1.2. Injured cardiomyocytes increased the use of carbon sources other than glucose

The total cellular concentration of ^{13}C labelled and unlabelled metabolites represents the contribution of different carbon sources to the metabolite. As shown in Fig. 2D, compared with control cells, the total cellular concentration of several metabolites in the TCA cycle (citrate/isocitrate, *cis*-aconitate, succinate, fumarate, and malate) of model cells was significantly increased, and the increase of metabolites in the upstream pathway (citrate/isocitrate and *cis*-aconitate) was greater than that in the downstream pathway (succinate, fumarate, and malate). Although m+2 isotopologues of succinate, fumarate, malate, and aspartate (representing oxaloacetate) were significantly decreased after treatment, their total cellular concentrations were all increased. As shown in Fig. 2A, glutamine is a source of carbon that enters the TCA cycle to supplement downstream metabolite levels. Our results indicated that the enhancement of glutamine oxidative carboxylation diluted the ^{13}C labelling ratio of these downstream metabolites. As shown in Fig. 2D (Table S2), the total cellular concentration of lactate, the end product of glycolysis, was increased after injury, which indicated that glycolysis was enhanced after ischemic injury. The total cellular concentration of pyruvate increased after injury, but its ^{13}C labelling ratio (m+3 isotopologue) decreased, which indicated that pyruvate produced from lipid and amino acid metabolism increased.

3.2. GBE monomers exhibit a significant protective effect on injured cardiomyocytes

According to a CCK-8 assay, the viability of ISO-injured cells was significantly lower than that of the control cells as shown in Fig. 3A (Table S3), which indicated that ISO caused significant injury. Bilobalide, ginkgolide B, kaempferol and rutin improved the cell viability influenced by ISO and showed significant protective effects on injured cardiomyocytes.

3.2.1. Regulation mitochondrial aerobic respiration by GBE monomers in injured cardiomyocytes

In the OCR analysis, which reflects mitochondrial aerobic respiratory function, basal respiration, ATP production, and maximal respiration were markedly decreased by ISO-induced injury (Figs. 3B (Tables S4-S6) and C). However, basal respiration and ATP production were elevated with bilobalide and apigenin treatment; maximal respiration was elevated with bilobalide, ginkgolide B, and apigenin treatment. These results showed that mitochondrial aerobic respiratory dysfunction occurred after ISO-induced injury. Both basal respiration, which shows cellular energetic demand under baseline conditions, and ATP production, which contributes to meeting cellular energetic needs, were impaired, but also maximal respiration, which shows the maximum rate of respiration that the cell can achieve, was markedly decreased. Among the prototypes used to treat the ISO-injured cells, bilobalide and apigenin significantly regulated all aerobic processes listed above and improved this crucial energy metabolism process. The combination of cell viability and Seahorse test data showed that bilobalide had a significant mitochondrial respiratory protective effect in cardiomyocytes.

3.2.2. Bilobalide modulated the TCA cycle flux in ISO-injured cardiomyocytes

As shown in Figs. 2A and B, bilobalide-treated cells had significant changes compared with the changes in the model cells: ^{13}C labelled metabolites in the upstream TCA cycle were significantly decreased, including m+2 isotopologues of citrate/isocitrate and *cis*-aconitate, whereas ^{13}C labelled metabolites in the downstream TCA cycle, including m+2 isotopologues of α-ketoglutarate, succinate, fumarate, malate, and aspartate (representing oxaloacetate), were significantly increased. This indicated that bilobalide released the accumulated citrate/isocitrate and *cis*-aconitate from glucose sources into the downstream pathway and modulated the flux of the TCA cycle. Intermediates flowed and were transformed more smoothly in bilobalide-treated ISO-injured cardiomyocytes than in untreated ISO-injured cardiomyocytes.

This was associated with changes in the activity of key metabolic enzymes. As shown in Fig. 2C, compared with the ratios of the model cells, the citrate m+2/pyruvate m+3 ratio was significantly decreased after bilobalide treatment, which indicated reduced PDH and/or CS activity after bilobalide treatment. Additionally, the α-ketoglutarate m+2/isocitrate m+2 ratio was significantly increased, which indicated an increase in IDH2 activity. This could also be caused by the decrease of upstream metabolites reducing the pressure on IDH2 because it is a rate-limiting enzyme in the TCA cycle.

The regulation of metabolic flux from glucose to the TCA cycle by bilobalide also affected the contribution from other carbon sources. As shown in Fig. 2D, bilobalide significantly reduced the total cellular concentrations of both upstream and downstream metabolites in the TCA cycle, including citrate/isocitrate, *cis*-aconitate, succinate, fumarate, malate, and aspartate (representing oxaloacetate). Due to these changes, ^{13}C labelled metabolites in the downstream TCA cycle from glucose were significantly increased compared with those in the model cells. This indicates that other carbon sources that flowed into the downstream TCA cycle were decreased with bilobalide treatment. It also suggests an effect of bilobalide in the modulation of TCA pathway flux and the reduction of the inflow of other carbon sources to maintain TCA cycle balance.

3.3. Key enzymes in energy metabolism related to MI and bilobalide activity

As shown in Figs. 4A and B (Table S7), enzyme expression levels indicated that the effects of ISO injury and bilobalide treatment on energy metabolic enzymes in cardiomyocytes were extensive. Compared to gene expression in the control cells, ISO-induced injury caused upregulated expression of many enzymatic genes, including PDH, CS, succinate-coenzyme A ligase (SUCLG), and succinate dehydrogenase (SDH), which were part of the key regulatory nodes found in the MFA results. Although there was no significant difference between treatments due to insufficient sample size, the mRNA expression levels after ISO-induced injury tended to be higher than those of the control cells, which was consistent with the results of the MFA. As shown in Fig. 4D (Figs. S2-S7), the protein expression levels of PDH and CS were significantly increased after ISO-induced injury, which was also consistent with the results of the MFA and PCR array. Similarly, the expression levels of SUCLG and SDH were increased after injury, which was consistent with the changes in the total cellular concentrations of succinate and fumarate. However, no obvious change was observed in the expression levels of IDH2 in ISO-injured cells, which was consistent with the result of the IDH2 activity test (Fig. 4C (Table S8)). IDH2 is a TCA cycle rate-limiting enzyme. Although its expression level and activity did not change in ISO-injured cells, upstream PDH and CS were significantly changed; thus, even if the upstream metabolites accumulated, IDH2 could not release them into the downstream TCA cycle rapidly, which blocks TCA cycle flux.

In the ISO-injured H9c2 cells protected by bilobalide, mRNA expression levels of the crucial metabolic enzymes, including PDH, CS, SUCLG, and SDH, tended to be lower than those of the ISO-induced cells. The protein expression levels of these energy metabolic enzymes were also significantly decreased, which was

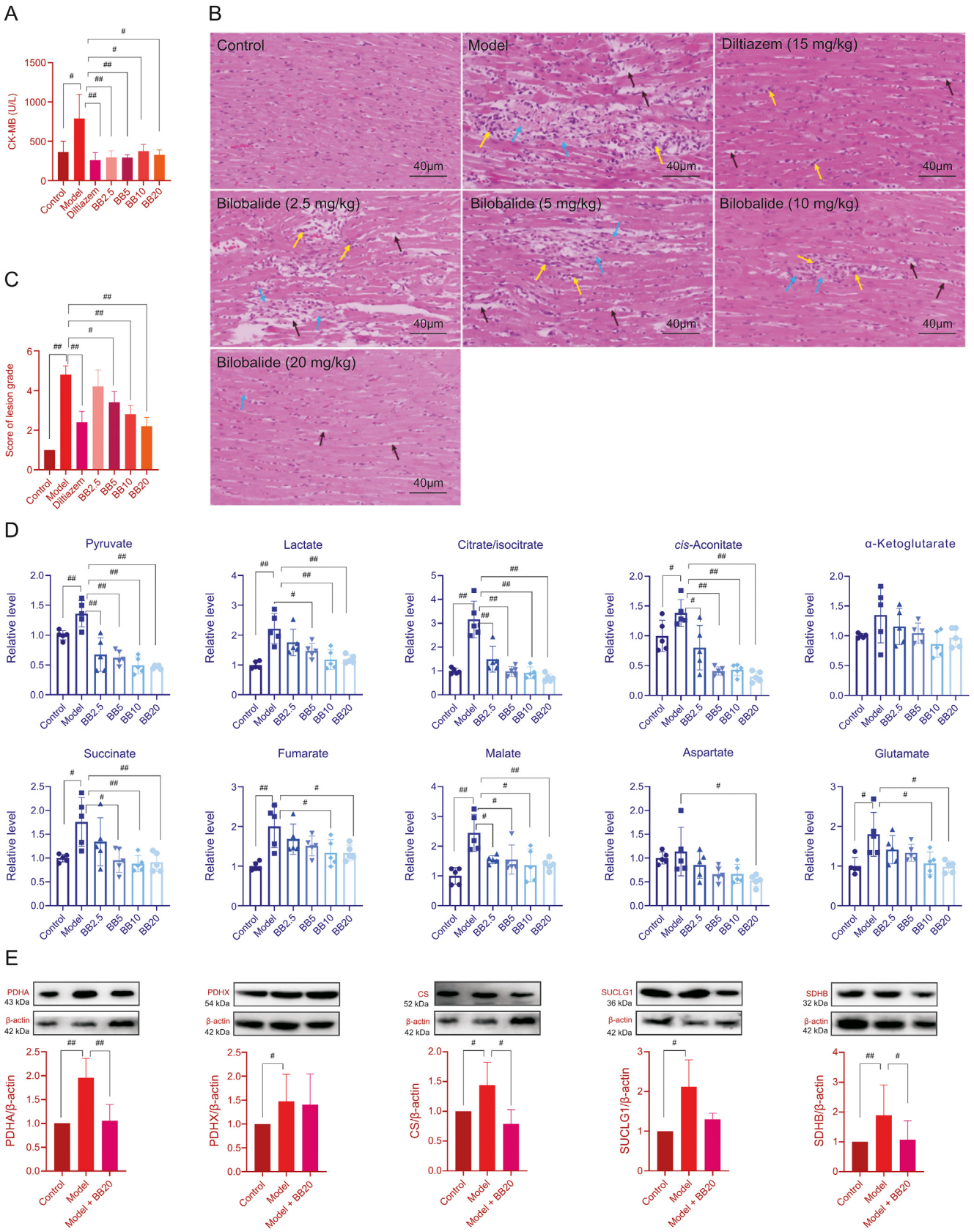

Fig. 5. (A) The content of heart enzyme creatine kinase-muscle brain (CK-MB) in rat plasma (n=5. The original data are shown in Table S9). (B) Histopathological examination of the myocardium (blue arrows: cardiomyocyte necrosis, muscle fibre rupture, and myofibrillar dissolution; black arrows: the space of cardiac muscle was widened; yellow arrows: infiltration of inflammatory cell). (C) Score of lesion grade in each rat group (score 1: no obvious lesions; black score 2: slight lesions; score 3: mild lesions; score 4: moderate lesions; score 5: severe lesions; n=5). (D) The content of metabolites in the energy metabolism pathway in rat myocardium (n=5. The original data are shown in Table S10). (E) The protein expression levels of PDH, CS, SUCLG, and SDH in rat myocardium (n=4–10. The original data are shown in Figs. S8–S12). Error bars represent mean ± SD, $^{\#}P < 0.05$, $^{\#\#}P < 0.01$. PDHA and PDHX are subunits of PDH. SUCLG1 is a subunit of SUCLG. SDHB is a subunit of SDH.

consistent with the MFA results. Although bilobalide did not change the expression and activity of IDH2, bilobalide treatment decreased the expression levels of upstream PDH and CS and downstream SUCLG and SDH, which reduced the accumulation of metabolites and the pressure on IDH2. Therefore, PDH, CS, SUCLG, and SDH, especially PDH and CS, were the key metabolic enzymes affected by ISO-induced injury, and bilobalide regulated their expression levels to improve the TCA cycle flux.

3.4. Bilobalide protected the impaired TCA cycle in MI rats

The TCA cycle flux-improving effect of bilobalide was verified in MI rats. As shown in Fig. 5A (Table S9), the level of myocardial enzyme CK-MB in the plasma of MI model rats was significantly increased compared to that of control rats, which indicated that MI injury led to cardiomyocyte damage and rupture. The myocardial enzyme was released into the blood, which indicated successful model establishment. Compared with that in the control group, the CK-MB level in diltiazem-treated rats was significantly decreased, which further supported the success of the model. Similarly, the CK-MB level in rats treated with different doses of bilobalide also showed a significant decrease compared with that of the MI model rats, indicating that bilobalide had a protective effect on the heart of MI rats. In addition, as shown in Figs. 5B and C, the histopathological examination of myocardial tissue from MI rats also showed typical ischemic injury symptoms, whereas the area and extent of injury were significantly reduced in the diltiazem and bilobalide pre-treated groups.

Fig. 5D (Table S10) shows the targeted metabolomic results of the myocardia of the control, model, and bilobalide pre-treated groups. Compared with the contents in the control group, the contents of citrate/isocitrate, *cis*-aconitate, succinate, fumarate, malate, glutamate, pyruvate, and lactate in the myocardia of the model group were significantly increased, especially the levels of citrate/isocitrate and *cis*-aconitate in the upstream pathway. This indicated that the TCA cycle was blocked between isocitrate and α-ketoglutarate, which was consistent with the results of the H9c2 cell experiments. Compared with the contents in the model group, the contents of the above metabolites and aspartate in the myocardia of bilobalide pre-treated groups were significantly decreased, especially with the bilobalide 20 mg/kg treatment, which suggested that bilobalide reduced the accumulation of metabolites and improved TCA cycle flux. This was also consistent with the results of the H9c2 cell experiments. As shown in Fig. 5E (Figs. S8-S12), the expression levels of PDH, CS, SUCLG, and SDH in rat myocardium were significantly increased after ISO-induced MI model group and decreased after 20 mg/kg bilobalide treatment, which was consistent with the results of the targeted metabolomics and H9c2 cell experiments.

4. Discussion

As a famous herbal medicine, GBE has been widely used in the prevention and treatment of IHD. This research on the mechanism and material basis of GBE's protective properties not only elucidates the pathogenesis of MI but also could help to develop new drugs. Previous studies reported that GBE contains two groups of active components: terpene lactones and flavonol glycosides [12]. Terpene lactones include bilobalide, ginkgolide A, B, C, M and J, which are unique components of GBE, and have antiplatelet activation and neuroprotective effects [12]. Flavonol glycosides mainly derive from the aglycones of quercetin, kaempferol, and isorhamnetin, which are secondary metabolites widely distributed in many plants that have antioxidant functions, vascular endothelial cell proliferation inhibiting effects, and aid in blood fat reduction [12]. Therefore, it was hypothesized that the significant MI protective effect of GBE was mainly derived from the unique terpene lactones and from the multi-target effect of flavonol glycosides.

This hypothesis was verified in our previous metabolomics study of GBE against MI in rats [11]. It was found that GBE significantly restores lipid (fatty acids, sphingolipid, phosphoglyceride and glyceride) metabolism disorders and amino acid and energy metabolism disorders in MI model rats. This is closely related to the antioxidant and lipid-lowering effects of flavonol glycosides and the antiplatelet activation of terpene lactones. The regulation of energy metabolism by GBE was of great interest to us because the heart is the organ that powers the circulatory system. The heart works continuously and needs to obtain enough energy to do so. The most direct effects of MI injury should impair energy metabolism. In our previous study, we observed that GBE significantly reduced the accumulation of citrate in the MI rat myocardium. Arginine, ornithine, and citrulline (in the urea cycle) and aspartate significantly increased after MI and were metabolized as intermediates to maintain the TCA cycle, whereas GBE significantly decreased their levels. Based on this result, we further focused on energy metabolism pathways, especially the TCA cycle, which is the hub of carbohydrate, lipid, and amino acid metabolism. Effects on the TCA cycle are probably the most important mechanism for GBE's protective effect against MI.

In this study, using a stable isotope tracing MFA technique and [U−^{13}C] glucose as a tracer, we found that the energy metabolic flux of ISO-injured cardiomyocytes had problems. Glucose as a source of carbon in the TCA cycle was blocked. A large amount of citrate/isocitrate and *cis*-aconitate accumulated upstream, and the proportions of these intermediates entering the downstream cycle were significantly decreased. The TCA cycle has multiple carbon sources, including glucose, fatty acids, and amino acids. These carbon sources enter the TCA cycle mainly through glycolysis, fatty acid oxidation, and glutamine oxidative and reductive carboxylation. The contribution of each of these carbon sources to the TCA cycle also affects the contributions of the others [8]. Therefore, in order to maintain an energy supply, cardiomyocytes enhance anaplerosis from other carbon sources, especially the increase of glutamine into the TCA cycle, resulting in the total cellular concentration of downstream metabolites still rising. However, increase in other carbon sources did not alleviate the blockage of the TCA cycle, and its metabolic flux became impaired and further increased the burden on the mitochondria in cardiomyocytes. This was apparent from the decrease of basal aerobic respiration and maximal aerobic respiratory capacity detected by the Seahorse test.

The tissue distribution experiment with GBE found nine prototypes in the rat myocardium that were used as candidates. Through the Seahorse test combined with the injured cardiomyocyte viability test, we found bilobalide to have a good protective effect on mitochondrial aerobic respiration in ISO-injured cardiomyocytes. Bilobalide improved both the direct output (ATP production and basal respiration) and the potential (maximal respiration) of aerobic respiration. Bilobalide is an important sesquiterpene in GBE. Due to its significant anti-ischemic and neuroprotective effects [19–23], it can be used to prevent and treat IHD [19], stroke [20], and Alzheimer's disease [21]. It has been reported that bilobalide has a protective effect on the mitochondria [19,20,22,23], including the protection of complex I and III activities [19,23], preservation of mitochondrial ATP synthesis [20], and increases the expression of the mitochondrial DNA-encoded COX III subunit of cytochrome C oxidase and ND1 subunit of NADH dehydrogenase [22]. However, these mechanisms did not explain the results of our previous experiment. GBE reduces large accumulation of TCA cycle intermediates. This is a regulation of the metabolic flux, which is different from the mechanisms previously reported.

Therefore, it was necessary to further this study from the perspective of cellular metabolic flux.

The MFA showed that bilobalide modulated the TCA cycle flux in injured cardiomyocytes. It significantly reduced the accumulation of citrate/isocitrate and *cis*-aconitate from glucose upstream, increased their amount entering downstream, balanced the utilization of different carbon sources, and reduced the intake of glutamine downstream. With bilobalide treatment, the metabolic flux of the TCA cycle was enhanced and the metabolic pressure on cardiomyocytes was decreased, which were apparent from the recovery of basic aerobic respiratory and maximal aerobic respiratory capacity. In addition, key metabolic sites were found. Based on the expression level of enzymes in these sites, an interesting finding was that the expression and activity of IDH2 at the blocked sites did not change significantly. Metabolic blocking was caused by the high expression of upstream enzymes PDH and CS after injury, while IDH2 is a rate-limiting enzyme of the TCA cycle. Excessive metabolite levels cannot enter the downstream cycle in time, resulting in a large amount of accumulation. Bilobalide downregulated the expression levels of PDH and CS. Additionally, downstream metabolic enzymes SUCLG and SDH were also targets of bilobalide. The results of these cell experiments were further confirmed in rats. Treatment of MI rats with bilobalide showed dose-dependent protection on myocardial tissue and regulation of the accumulation of TCA cycle intermediates. Moreover, regulation effects of bilobalide on PDH, CS, SUCLG, and SDH were also observed. The above results are summarized in Fig. 6.

The TCA cycle plays an important role in metabolism. It is not only the hub for carbohydrate, lipid, and protein metabolism but also provides most of the energy for biological activities. The fluency of TCA cycle is very important for maintaining normal cellular function, especially energy output. Although bilobalide has been reported to protect mitochondrial aerobic respiration through different mechanisms [19,20,22,23], this is the first time its effect in improving TCA cycle flux has been reported. This provides a new way to treat IHD. In addition, after ISO-induced ischemia-like injury, glycolysis in cardiomyocytes was significantly enhanced, gene expression of metabolic enzymes was upregulated, and the content of lactate was significantly increased, which could lead to cellular acidosis. In this case, H^+ is pumped out of the cell and Ca^{2+} is pumped in, causing intracellular Ca^{2+} overload and exacerbating myocardial damage [3,24]. Under the protection of bilobalide, the glycolysis in cardiomyocytes was significantly weakened, gene expression of related metabolic enzymes was downregulated and accumulation of lactate significantly decreased. Bilobalide reduced the accumulation of citrate/isocitrate and *cis*-aconitate, and it also weakened glycolysis and other carbon sources metabolized into intermediates of TCA cycles. All these effects relieved further reduction in mitochondrial pH.

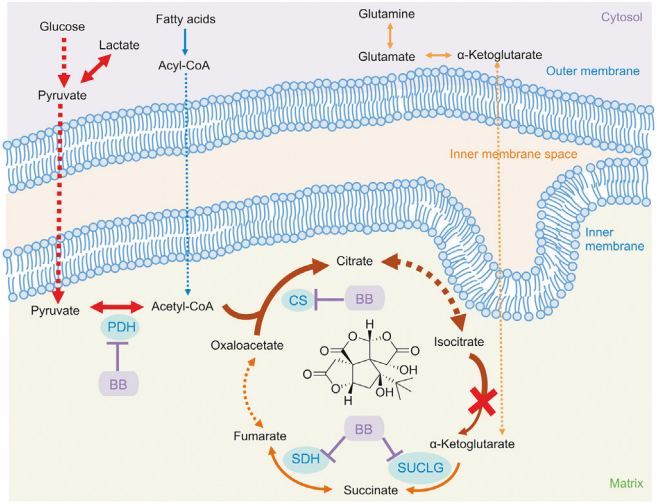

Fig. 6. Mechanism of bilobalide protecting energy metabolism of ischemic cardiomyocytes. Arrow color represents different carbon sources. Arrow thickness represents the flux change after ischemia.

Above all, bilobalide was identified as an active ingredient of GBE protecting ISO-injured ischemia-like cardiomyocytes by rescuing impaired TCA cycle flux and enhancing mitochondrial aerobic respiration. Other active components in GBE, including other terpene lactones and flavonol glycosides, also play a synergistic role through antioxidant function, antiplatelet activation, blood fat reduction, and vascular endothelial cell proliferation inhibition, making GBE a multi-targeted therapy. Bilobalide, which had a unique mechanism different from those of previous myocardial energy metabolism drugs, is expected to be a new drug in the future.

5. Conclusions

In this study, we investigated the mechanism of TCA cycle flux blocking in ISO-induced MI and further elaborated the mechanism and material basis of the anti-MI effect of GBE. Through MFA, it was found that ISO-injured cells experienced a blockage of carbon flow from glycolysis to the TCA cycle and enhanced anaplerosis from other carbon sources. In the Seahorse test, bilobalide was found to have a positive effect on the modulation of mitochondrial aerobic respiration. Bilobalide also significantly modulated the TCA cycle flux, reduced abnormal metabolite accumulation, and balanced the demand from carbon sources. It was realized by decrease in the enhanced expression of key metabolic enzymes in injured cells. This efficacy of bilobalide was verified in experiments in a rat model of MI. The results associated with treatment with bilobalide, an active compound of GBE, are not only further proof of the pathological metabolic mechanism of MI, but also provide inspiration for new drug discovery. This study shows the advantages and potential of combining the Seahorse test with MFA techniques to serve as a powerful strategy for future research on the mechanisms of herbal medicine based on metabolomic results.

Declaration of competing interest

The authors declare there are no conflicts of interest.

Acknowledgments

This work was supported by grants from the National Natural Science Foundation of China (Grant No.: 81803496), the CAMS Innovation Fund for Medical Sciences (Grant No.: 2016-I2M-3-016), and the Applications and Core Technology University Research (ACT-UR, Grant No.: 4084).

Appendix A. Supplementary data

Supplementary data to this article can be found online at https://doi.org/10.1016/j.jpha.2020.08.008.

References

[1] P.C. Rezende, F.F. Ribas, J.C.V. Serrano Jr., et al., Clinical significance of chronic myocardial ischemia in coronary artery disease patients, J. Thorac. Dis. 11 (2019) 1005–1015.

[2] R.R. Aguiar, D.F. Vale, R.M.D. Silva, et al., A possible relationship between gluconeogenesis and glycogen metabolism in rabbits during myocardial ischemia, An. Acad. Bras. Cienc. 89 (2017) 1683–1690.
[3] Q. Liu, J.C. Docherty, J.C. Rendell, et al., High levels of fatty acids delay the recovery of intracellular pH and cardiac efficiency in post-ischemic hearts by inhibiting glucose oxidation, J. Am. Coll. Cardiol. 39 (2002) 718–725.
[4] G.M. Rosano, M. Fini, G. Caminiti, Cardiac metabolism in myocardial ischemia, Curr. Pharmaceut. Des. 14 (2008) 2551–2562.
[5] G.D. Lopaschuk, Metabolic modulators in heart disease: past, present, and future, Can. J. Cardiol. 33 (2017) 838–849.
[6] B.S. Kalra, V. Roy, Efficacy of metabolic modulators in ischemic heart disease: an overview, J. Clin. Pharmacol. 52 (2012) 292–305.
[7] H. Brunengraber, C.R. Roe, Anaplerotic molecules: current and future, J. Inherit. Metab. Dis. 29 (2006) 327–331.
[8] G. Czibik, V. Steeples, A. Yavari, et al., Citric acid cycle intermediates in cardioprotection, Circ. Cardiovasc. Genet. 7 (2014) 711–719.
[9] J. Tian, Y. Liu, K. Chen, Ginkgo biloba extract in vascular protection: molecular mechanisms and clinical applications, Curr. Vasc. Pharmacol. 15 (2017) 532–548.
[10] P. Allawadhi, A. Khurana, N. Sayed, et al., Isoproterenol-induced cardiac ischemia and fibrosis: plant-based approaches for intervention, Phytother Res. 32 (2018) 1908–1932.
[11] Z. Wang, J. Zhang, T. Ren, et al., Targeted metabolomic profiling of cardioprotective effect of *Ginkgo biloba* L. extract on myocardial ischemia in rats, Phytomedicine 23 (2016) 621–631.
[12] M.R. Antoniewicz, Methods and advances in metabolic flux analysis: a mini-review, J. Ind. Microbiol. Biotechnol. 42 (2015) 317–325.
[13] M.R. Antoniewicz, A guide to 13 C metabolic flux analysis for the cancer biologist, Exp. Mol. Med. 50 (2018) 1–13.
[14] D.T.H. Leung, S. Chu, Measurement of Oxidative Stress: Mitochondrial Function Using the Seahorse System, in: Preeclampsia, Humana Press, New York, 2018, pp. 285–293.
[15] C.J. Halbrook, C. Pontious, I. Kovalenko, et al., Macrophage-released pyrimidines inhibit gemcitabine therapy in pancreatic cancer, Cell Metab. 29 (2019) 1390–1399.e6.
[16] J.R. Molina, Y. Sun, M. Protopopova, et al., An inhibitor of oxidative phosphorylation exploits cancer vulnerability, Nat. Med. 24 (2018) 1036–1046.
[17] D. Menon, R. Coll, L.A. O'Neill, et al., GSTO1-1 modulates metabolism in macrophages activated through the LPS and TLR4 pathway, J. Cell Sci. 128 (2015) 1982–1990.
[18] K.D. Courtney, D. Bezwada, T. Mashimo, et al., Isotope tracing of human clear cell renal cell carcinomas demonstrates suppressed glucose oxidation in vivo, Cell Metab. 28 (2018) 793–800.e2.
[19] D. Janssens, E. Delaive, J. Remacle, et al., Protection by bilobalide of the ischaemia-induced alterations of the mitochondrial respiratory activity, Fund. Clin. Pharmacol. 14 (2000) 193–201.
[20] T.M. Schwarzkopf, K.A. Koch, J. Klein, Neurodegeneration after transient brain ischemia in aged mice: beneficial effects of bilobalide, Brain Res. 1529 (2013) 178–187.
[21] F. Tchantchou, P.N. Lacor, Z. Cao, et al., Stimulation of neurogenesis and synaptogenesis by bilobalide and quercetin via common final pathway in hippocampal neurons, J. Alzheim. Dis. 18 (2009) 787–798.
[22] F.V. Defeudis, Bilobalide and neuroprotection, Pharmacol. Res. 46 (2002) 565–568.
[23] Z. Feng, Q. Sun, W. Chen, et al., The neuroprotective mechanisms of ginkgolides and bilobalide in cerebral ischemic injury: a literature review, Mol. Med. 25 (57) (2019) 1–8.
[24] H. Kahles, M.M. Gebhard, V.A. Mezger, et al., The role of ATP and lactic acid for mitochondrial function during myocardial ischemia, Basic Res. Cardiol. 74 (1979) 611–620.